Creep Data Analyses of a Columnar-Grained Nickel-Base Superalloy by Conventional and β-Envelope Methods

M.S. Gopala Krishna, A.M. Sriramamurthy, and V.M. Radhakrishnan

(Submitted 18 September 1997; in revised form 5 March 1998)

Creep-rupture properties of a columnar-grained nickel-base superalloy have been evaluated over a wide temperature range (1033 to 1311 K) and stress levels (80 to 850 MPa). Creep data analyses based on the conventional approach as well as on a new graphical method—the β-envelope method (Ref 1)—have been carried out for creep strain and life estimation purposes. The relation between minimum creep rate of the alloy with the applied stress obeys simple power law, whereas the rupture data of the alloy fits well to the Larson-Miller parameter. Also, the Monkman-Grant relation between the minimum creep rate and the rupture life produces a trend with some degree of scatter in the data. The latter relation in its generalized form by the β-envelope method exhibited the best correlation with significantly reduced scatter in the data.

Keywords β-envelope method, creep, minimum creep rate, nickel-base superalloy, rupture life

1. Introduction

1.1 β-Envelope Method

Recently, a procedure known as the β-envelope method has been developed to analyze the creep behavior of high-temperature materials (Ref 1-5). The β-envelope method has several advantages over the theta (θ) projection method (Ref 6), as detailed in Ref 1. With this method, the creep strain, ε, and time, *t*, in the three stages of primary, secondary, and tertiary creep are enveloped by three straight lines on the log-log scale, as shown schematically in Fig. 1. The enveloping lines are described by the following equations:

$$\varepsilon_1 = \beta_1 t^{x_1}$$

$$\varepsilon_2 = \beta_2 t^{x_2}$$

and

$$\varepsilon_3 = \beta_3 t^{x_3} \quad \text{(Eq 1)}$$

where β_1, β_2 and β_3 are the coefficients. The subscripts 1, 2, and 3 denote the first, second, and third stages of creep deformation, respectively. The values of the exponents x_1, x_2, and x_3 are, respectively, 1/3, 1, and 3 for most of the metallic materials. Because each equation describes the data points in each region separately, the coefficient in each region is not affected by the data points in the other two regions. At the transition from stage 1 to stage 2:

$$\beta_1 t_{12}^{1/3} = \varepsilon_{12} \quad \text{(Eq 2)}$$

and

$$\beta_2 t_{12} = \varepsilon_{12} \quad \text{(Eq 3)}$$

where the subscript 12 refers to a point at the intersection of the primary and secondary lines. The time t_{12} corresponds to the end of the first stage and the beginning of the second stage and is given by:

$$t_{12} = \left(\frac{\beta_1}{\beta_2}\right)^{3/2} \quad \text{(Eq 4)}$$

Similarly,

$$\beta_2 t_{23} = \varepsilon_{23} \quad \text{(Eq 5)}$$

$$\beta_3 t_{23}^3 = \varepsilon_{23} \quad \text{(Eq 6)}$$

which leads to

$$t_{23} = \sqrt{\frac{\beta_2}{\beta_3}} \quad \text{(Eq 7)}$$

Thus, the boundary times of the first and the second stage creep, namely t_{12} and t_{23}, are defined in terms of the coefficients β_1, β_2,

M.S. Gopala Krishna and **A.M. Sriramamurthy,** Defence Metallurgical Research Laboratory, Hyderabad-500058, India; and **V.M. Radhakrishnan,** Department of Metallurgical Engineering, I.I.T., Madras-600036, India.

and β_3. Taking the cube of Eq 5 and then dividing by Eq 6 results in:

$$\frac{\beta_2^3}{\beta_3} = \varepsilon_{23}^2 \quad \text{(Eq 8)}$$

Now, taking the creep-rupture time and the creep-rupture strain as t_r and ε_r, one obtains:

$$\beta_3 t_r^3 = \varepsilon_r \quad \text{(Eq 9)}$$

Noting that the coefficient β_2 represents the minimum creep rate, $\dot{\varepsilon}_{min}$, Eq 10 becomes

$$\frac{\beta_2^3}{\beta^2} = \varepsilon_{23}^2 = \frac{\dot{\varepsilon}_{min}^3}{\beta_3} \quad \text{(Eq 10)}$$

and the latter with Eq 10 results in

$$\dot{\varepsilon}_{min} \cdot t_r = \left(\varepsilon_{23}^2 \cdot \varepsilon_r\right)^{1/3} \quad \text{(Eq 11)}$$

Thus, the product, $\dot{\varepsilon}_{min} \cdot t_r$ is dependent on ε_{23} and ε_r. If ε_{23} and ε_r are constant and independent of the stress level or rupture time, then the Monkman-Grant relation would result. However, in many cases, the creep strains ε_{23} and ε_r decrease with decreasing stress level. In such cases (Ref 2), the above relation correlates well with the minimum creep rate and rupture time.

1.2 Cast Nickel-Base Superalloys

Cast nickel-base superalloys are used extensively for manufacturing turbine blades for aeroengine applications. Modern aeroengines use air-cooled columnar-grained and/or single-crystal blades because these components withstand higher gas inlet temperatures compared to their equiaxed counterparts, thereby resulting in improved turbine efficiency. These components generally are produced by the directional solidification process (Ref 7). Modern gas turbines operate very close to $0.8 - 0.9T_m$, where T_m is the absolute incipient melting point of the turbine blade material used. In this temperature range, creep is one of the primary design considerations for the turbine blade. The severity of the operating conditions makes it necessary for the blade material to exhibit high resistance to creep deformation and fracture so that the required design lives of the component can be achieved. The long-time dimensional stability and design life estimates of the turbine blade generally are based on short-time laboratory creep data obtained on the blade material.

In the present study, the longitudinal creep properties of a cast nickel-base superalloy with a columnar grain structure were evaluated at 1033, 1143, 1253, and 1311 K at four stress levels for each test temperature. Creep analyses on the data were carried out by conventional and β-envelope methods. The results obtained are presented in the present paper.

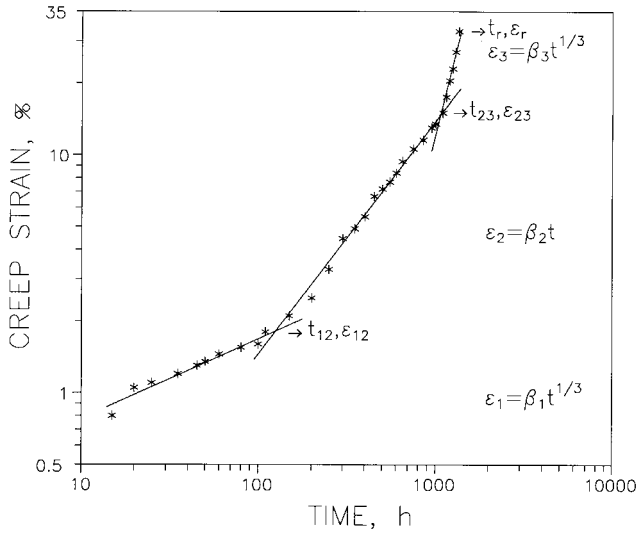

Fig. 1 Schematic representation of creep curve indicating the three stages of creep strain and the transition regions

2. Experimental

CM 247 LC is a cast nickel-base superalloy and is the proprietary alloy designation of M/s. Cannon Muskegon Corporation, USA, with a nominal chemical composition (wt%) of 8.3 Cr, 9.3 Co, 9.5 W, 3.2 Ta, 5.5 Al, 0.75 Ti, 1.5 Hf, 0.5 Mo, 0.015 Zr, 0.075 C, 0.015 B, and the balance Ni. The alloy is precipitation hardenable with 65 vol% $Ni_3(Al,Ti)(\gamma')$ precipitates in the matrix and commonly is used in columnar grain structures for turbine blade applications.

Rod samples 12 mm in diameter of the test alloy with a columnar grain structure were obtained by directional solidification. The process details and the heat treatment schedule adopted for production of the alloy are described in Ref 8. The rod samples were machined into round specimens and used for creep studies. Creep-rupture studies were carried out at 1033, 1143, 1253, and 1311 K at four stress levels at each test temperature. ATS direct-loading creep-testing machines fitted with three zone tubular furnaces were used in the study with a temperature stability of ±2 K. Creep strains on the specimens were measured to an accuracy of ±2 μm using two linear variable differential transducers fitted to the ends of a rod-in-tube type of extensometer mounted on the specimens. Results were recorded continuously on a strip chart recorder. The recorded raw data subsequently were converted into engineering creep curves.

3. Results and Discussion

The basic creep curves obtained for the alloy at 1003, 1143, 1253, and 1311 K and at various stress levels are shown in Fig. 2. The temperature range (1033 to 1311 K) over which the creep studies were carried out covered low-, intermediate-, and high-temperature regimes for the alloy in turbine applications. A rupture time range of 20 to 2500 h was observed in the study. At 1033 K, the creep curves exhibited a distinct but

short primary creep stage and a very limited tertiary stage for most of the stress levels used. However, secondary stage creep occurs very early in the deformation at other test temperatures and is followed by nonlinear creep strain accumulation with respect to time. The latter occupies a considerable amount of the total rupture time at all the test temperatures and stress levels, particularly above 1033 K. The total accumulated creep strain ranges from 5% at 1033 K to about 16% at 1311 K, i.e., strain to fracture increased with increasing temperature for the alloy. Creep fracture strain, e_f, has been found to be more dependent on temperature and to a lesser extent on applied stress.

Table 1 Power law relation between minimum creep rate and applied stress at various creep test temperatures

Temperature, K	Power law equation(a) $\dot{e}_{min} = A_1\sigma^n$	
	A_1	n
1033	1.727×10^{-49}	15.7
1143	6.077×10^{-20}	5.9
1253	1.469×10^{-19}	6.6
1311	4.600×10^{-20}	7.3

(a) $\dot{e}$ in h^{-1} and σ in MPa

The minimum creep rate determines the service life of a engineering structure/component. The minimum creep rate can be correlated with the applied stress at the test temperatures, as shown in Fig. 3 on a log-log plot. The relationship observed over the temperature range studied is governed by power law of the form:

$$\dot{e}_{min} = A_1\sigma^n \quad \text{(Eq 12)}$$

where A_1 is a temperature-dependent constant and n is the creep exponent. The values of the creep exponent, n, and A_1 at each test temperature are given in Table 1 and can be used to compute the

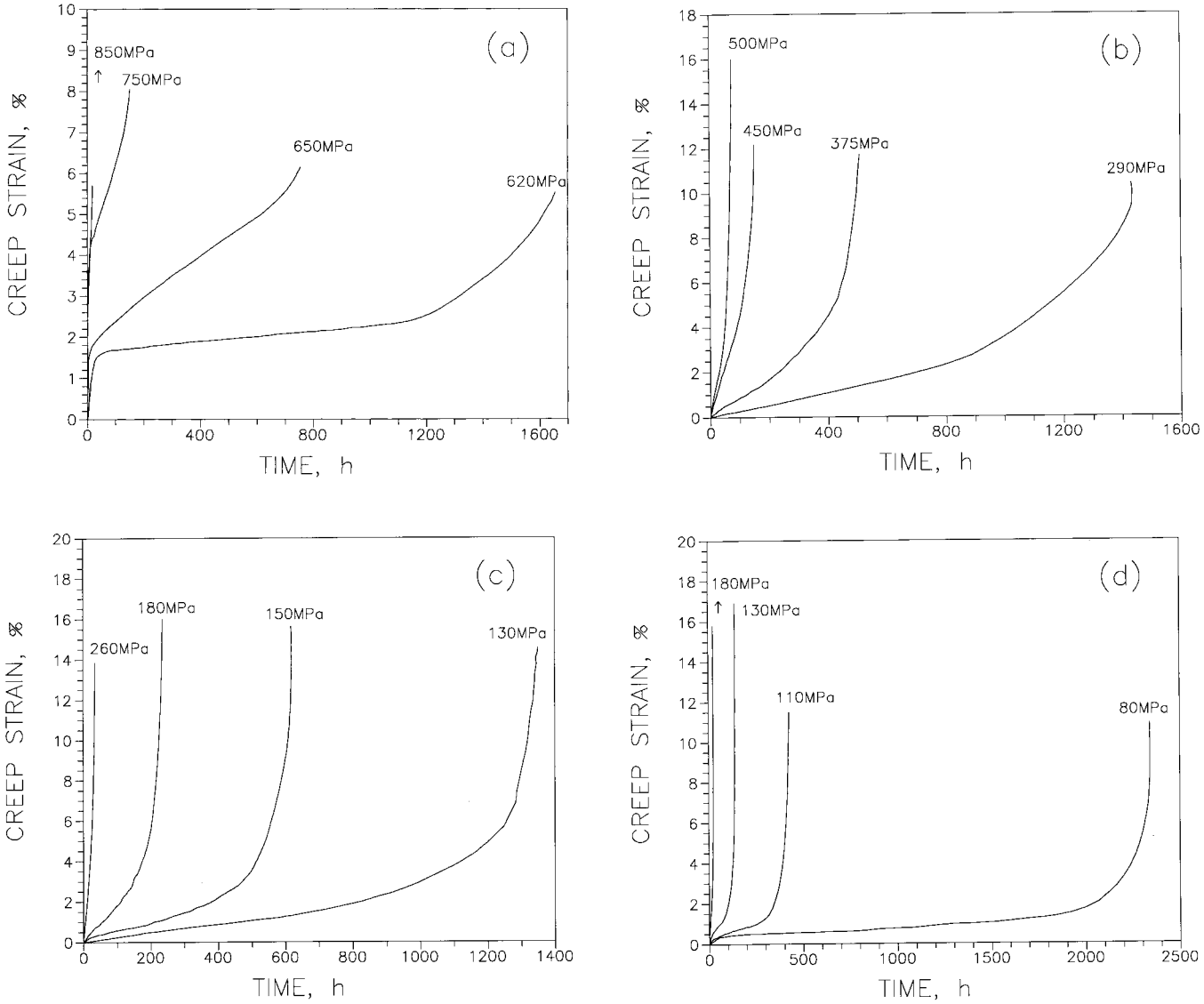

Fig. 2 Basic creep curves for the alloy at (a) 1033 K, (b) 1143 K, (c) 1253 K, and (d) 1311 K

minimum rate at other stress levels. In this study, n values were found to be in the range of 16 to 6. Such a high range of creep exponent suggests that dislocation creep may be the most dominant creep mechanism for this alloy. Similarly, the variation in rupture time with the applied stress at the test temperatures is shown in Fig. 4 on a log-log plot. The relation obtained is of the form:

$$t_r = A_2 \sigma^{-n'} \quad \text{(Eq 13)}$$

where A_2 is a temperature-dependent constant and n' is the exponent. The values A_2 and n' for the test alloy are listed in Table 2 for each of the test temperatures. The rupture time can be estimated for other stress levels. The values of the exponent, n', in the above relation are somewhat lower than those observed for the creep exponent. The values are in the range of 14 to 5. The trend in the exponent value follows the same pattern as in the case of minimum creep rate equation.

Under intergranular creep conditions, it is often observed that the steady state or minimum creep rate, $\dot{\varepsilon}_{min}$, and the rupture time, t_r, can be related by the Monkman-Grant relation:

$$\dot{\varepsilon}_{min} \cdot t_r = C_{MG} \quad \text{(Eq 14)}$$

Table 2 Power law relation between rupture life and applied stress at various creep temperatures

Temperature, K	Power law equation(a) $t_r = A_2\sigma^{-n'}$	
	A_2	n'
1033	6.554×10^{41}	13.80
1143	3.855×10^{16}	5.43
1253	3.244×10^{14}	5.37
1311	1.052×10^{14}	5.50

(a) t_r in h and σ in MPa

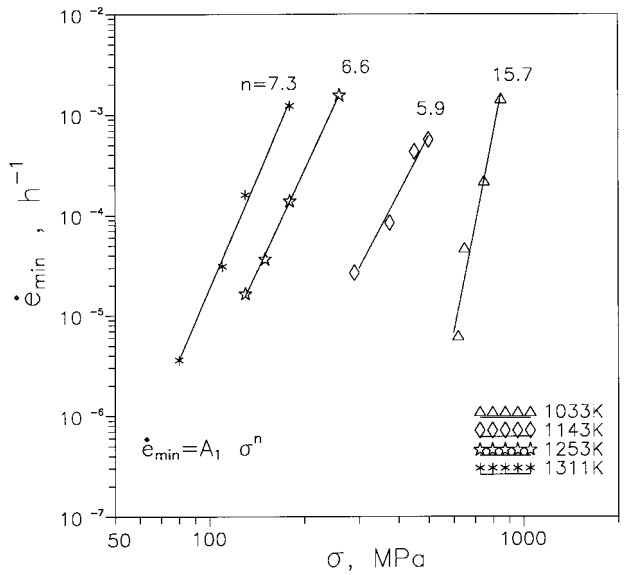

Fig. 3 Relation between minimum creep rate and applied stress

where C_{MG} is the Monkman-Grant constant, which lies in the range of 0.05 to 0.5 for many metals and alloys. The relation obtained for the test alloy is shown in Fig. 5. There appears to be some degree of scatter in the test data. A log-log least-squares fitting to the data points resulted in a slope of –1.18 and C_{MG} equal to 0.08 for the test alloy. Dobes and Millicka (Ref 9) have suggested that the scatter of data in the above relationship can be minimized by introducing the creep strain at fracture as a normalizing factor, thus leading to a modified Monkman-Grant relation of the form:

$$\frac{\dot{\varepsilon}_{min} \cdot t_r}{e_f} = C_{MMG} \quad \text{(Eq 15)}$$

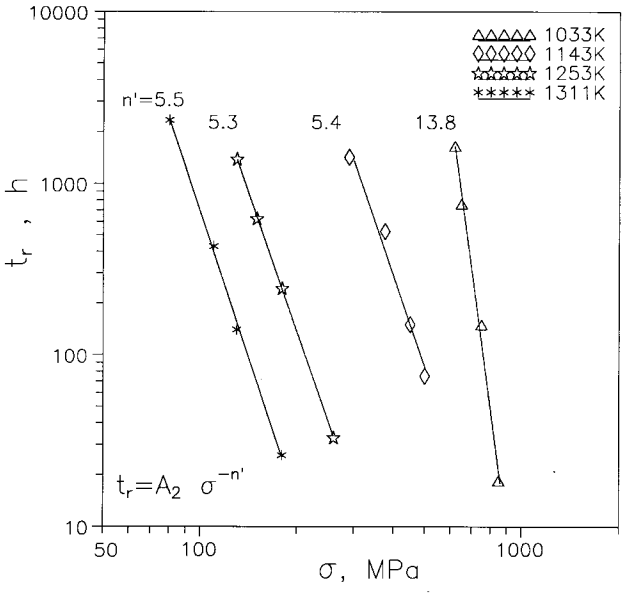

Fig. 4 Relation between rupture life and applied stress

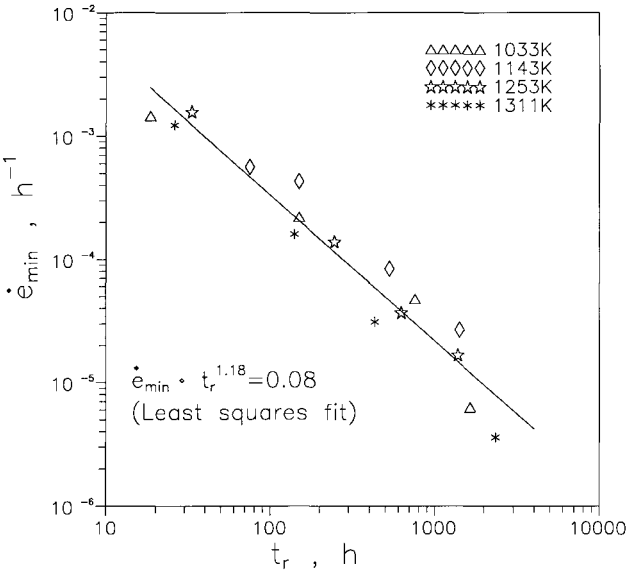

Fig. 5 Monkman-Grant relation

where C_{MMG} is the modified Monkman-Grant constant. By taking the creep fracture strain, e_f, as that measured over the gage length, the equation has been computed and the relation between the normalized strain rate ($\dot{e}_{min}/e_f$) and the rupture time is shown in Fig. 6 for the alloy along with least-squares fitted power law equation governing the data. However, even on normalizing the minimum creep rate data with the fracture strain, there is no improvement in the data scatter compared to the Monkman-Grant relation, as shown in Fig. 6. The latter was also evident on comparison of the correlation coefficient for the fits in Fig. 5 and 6, which were found to be 0.93 and 0.91, respectively. Hence, possibly with a factor of safety in design considerations, the Monkman-Grant relation itself can be used to predict the rupture life of the test alloy for a specified minimum creep rate.

To predict long-time rupture life using the parametric approach from short-time rupture data, many parameters are used, of which the Larson-Miller parameter (P_{LM}) is the simplest and most widely used in the literature. This has been computed and shown in Fig. 7 for the test alloy. It is evident that very good correlation has been obtained between the experimental data and the Larson-Miller parameter. Thus, the P_{LM} parameter can be used to predict the long-time rupture life at a specified temperature and at different stress levels for the alloy.

The creep data on the test alloy were analyzed using the β-envelope method. Figure 8 illustrates the percent creep strain and time relation at 1143, 1253, and 1311 K, respectively, for the test alloy. In all of the cases, the primary stage is not distinctly pronounced, whereas the secondary and tertiary stages can be represented by two straight lines on a log-log scale. In the log-log least-squares fittings to the experimental data points of the basic creep curves, the slopes of the lines were found to be between 0.9 to 1.0 and 2.9 to 3.2 and can be approximated to 1 and 3, respectively, for the secondary and tertiary stages of creep deformation for the test alloy. Thus, the second and third stage creep strains, respectively, obey the equations

$$\varepsilon_2 = \beta_2 t \quad \text{(Eq 16)}$$

$$\varepsilon_3 = \beta_3 t^3 \quad \text{(Eq 17)}$$

The relationships between the coefficients β_2 and β_3 and the applied stress are shown in Fig. 9 and 10. The relations obtained can be given as:

$$\beta_2 = \beta_{2o}\sigma^p \exp\left(\frac{-Q_2}{RT}\right) \quad \text{(Eq 18)}$$

Table 3 Exponents and coefficients obtained in the secondary and tertiary stages of creep using the β-envelope method

Temperature, K	p	q	$\beta_{2o}\exp(-Q_2/RT)$	$\beta_{3o}\exp(-Q_3/RT)$
1143	6.3	16.7	9.602×10^{-21}	9.927×10^{-53}
1253	6.2	16.3	1.497×10^{-19}	1.857×10^{-45}
1311	6.7	17.5	1.200×10^{-17}	1.975×10^{-45}

$$\beta_3 = \beta_{3o}\sigma^q \exp\left(-\frac{Q_3}{RT}\right) \quad \text{(Eq 19)}$$

The linear relation on a log-log scale clearly indicates that a simple power law governs secondary and tertiary stages of creep deformation of this nickel-base superalloy in the stress and temperature range studied. The values of the stress exponents p and q and the variation of β_{2o} and β_{3o} as a function of temperature in the above equations are given in Table 3. These relations can be used to estimate creep strains at different stress levels and lives at various test temperatures used in the study.

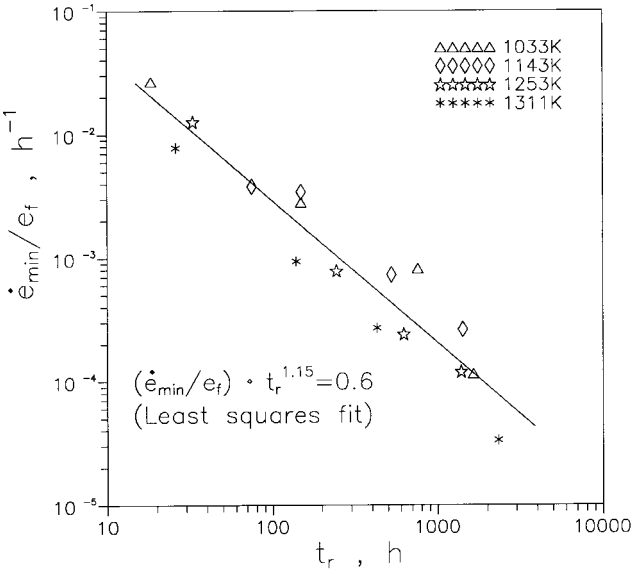

Fig. 6 Modified Monkman-Grant relation

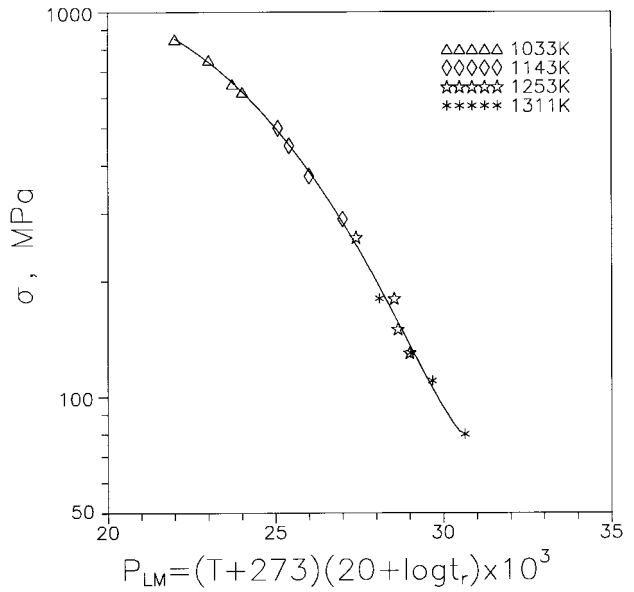

Fig. 7 Relation between applied stress and Larson-Miller parameter

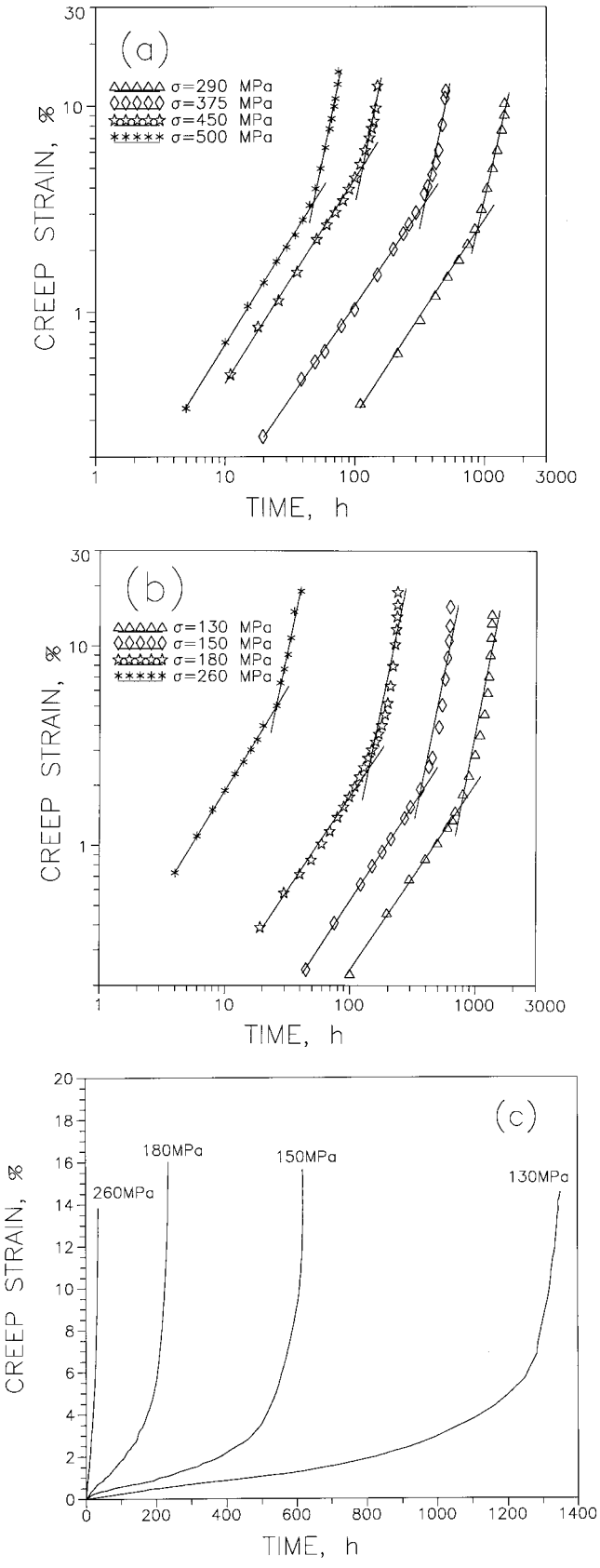

Fig. 8 Relation between creep strain and time on a log-log scale for the secondary and tertiary stages of creep at (a) 1143 K, (b) 1253 K, and (c) 1311 K

Also, the relationship between the minimum creep rate and rupture time obtained with the β-envelope method was given in Eq 13 and the same was computed for data on the test alloy. The results obtained are shown in Fig. 11 with a least-squares fitted equation governing the relation. Note that the scatter in data is reduced significantly compared to the Monkman-Grant relation or its modification as shown earlier in Fig. 5 and 6. The correlation coefficient for this fit was found to be 0.97 compared to 0.93 and 0.91 for the Monkman-Grant relation and its modified forms. From Fig. 11, it should be noted that the line passes nearly through the ordinate 1, thereby illustrating the applicability of Eq 13 to the alloy in the present analysis. Similar results have been reported (Ref 10) on cold worked AISI 316 N stainless steel used in nuclear reactor applications.

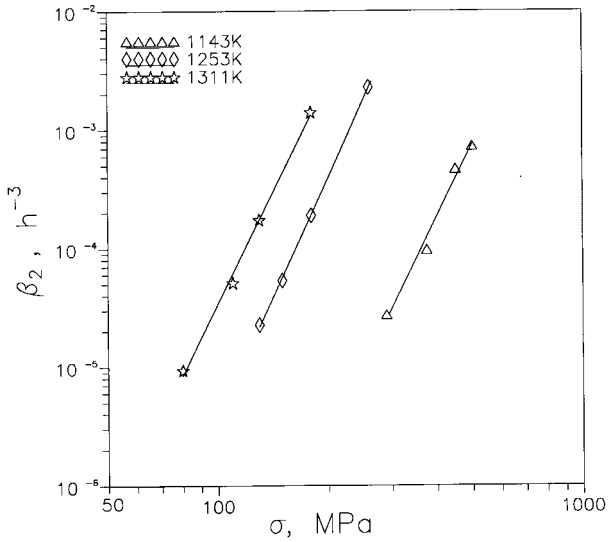

Fig. 9 Relation between β_2 and applied stress using the β-envelope method

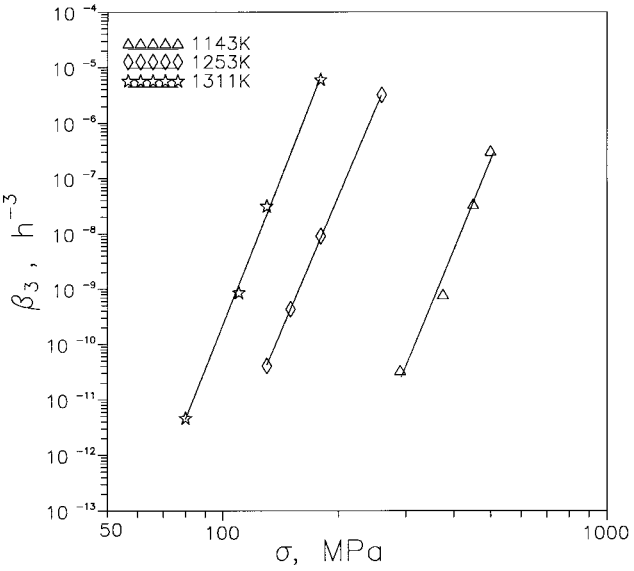

Fig. 10 Relation between β_3 and applied stress using the β-envelope method

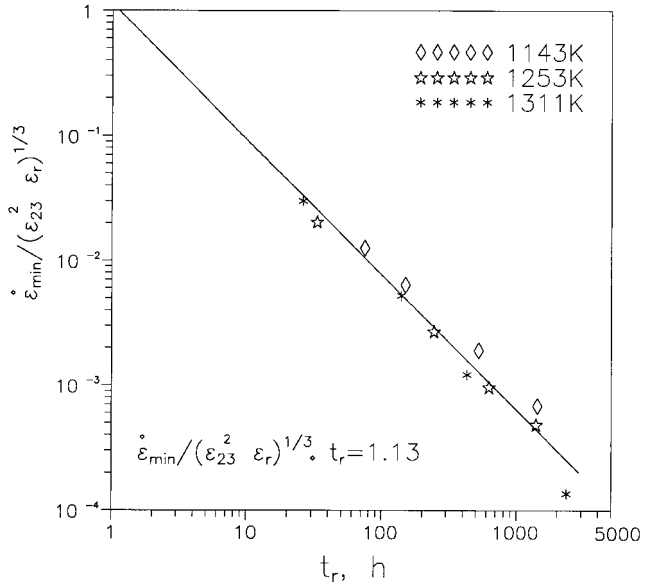

Fig. 11 Relation between rupture life and minimum creep rate using the β-envelope method

4. Conclusions

From the creep data analyses carried out over the temperature and stress level ranges for the test alloy, the following conclusions have been drawn. Short primary stage and dominant secondary stage creep was observed at 1033 K, whereas predominantly secondary and tertiary stages occurred at 1143, 1253, and 1311 K. The tertiary stage occupied a significant portion of the rupture life in the latter cases.

The dependence of minimum creep rate on applied stress can be described by Norton's power law of the form:

$$\dot{e}_{\min} = A_1\sigma^n$$

whereas the stress dependence of rupture time can be represented by the relation:

$$t_r = A_2\sigma^{-n'}$$

The values of the constants in these relations have been established at test temperatures for the test alloy.

The Monkman-Grant relation was obeyed by the test alloy with some apparent scatter in the data. No significant improvement in the scatter of the data was observed in a modified form of the relation. On parametric analysis of the rupture data, it is observed that the Larson-Miller parameter fit well to the data and hence can be used to predict the long-time rupture behavior from short-time rupture data on the alloy.

Using the β-envelope method, a graphical method of analyzing creep curves resulted in simple power relations for secondary and tertiary stages of creep for the test alloy. These relations can be used to predict the secondary and tertiary creep behavior of the test alloy over the temperature and stress level ranges studied.

Also, in the above analysis, the minimum creep rate and rupture life were related through creep strains at the onset of the tertiary stage and at rupture as given by Eq 11. Reduction in the scatter of the test data observed using this relation is excellent compared to the Monkman-Grant relation and its modified form.

Acknowledgments

The authors gratefully acknowledge the financial support received from the Defence Research Development Organisation (DRDO), New-Delhi, India, for carrying out the research work. Also, M.S. Gopala expresses sincere thanks to the Creep Group, DMRL, Hyderabad, for offering use of the facilities to carry out the creep studies on the test material.

References

1. V.M. Radhakrishnan, P.J. Ennis, and H. Schuster, "An Analysis of Creep Deformation and Rupture by the β-Envelope Method," KFA-Julich Report, No. 2535, Oct 1991
2. V.M. Radhakrishnan, *J. Mater. Eng. Perform.*, Vol 1, 1992, p 123
3. V.M. Radhakrishnan, Characterisation of Creep Deformation of a Ni-Base Superalloy, *Proc. 10th Congress on Materials Testing*, 1991, E. Czoboly, Ed., Scientific Society of Mechanical Engineers, Budapest, Hungary, p 94
4. V.M Radhakrishnan, *Fatigue, Fract. Eng. Mater. Struct.*, Vol 15 (No. 6), 1992, p 617
5. V.M. Radhakrishnan, *Mater. Sci. Technol.*, Vol 7, 1991, p 541
6. R.W. Evans, J.D. Parker, and B. Wilshire, Recent Advances in Creep and Fracture of Engineering Materials and Structures, B. Wilshire and D.R.J. Oswsen, Ed., Pineridge Press, Swansea, UK, 1982, p 135
7. F.L. Versnyder and M.E. Shank, *Mater. Sci. Eng.*, Vol 7, 1970, p 213
8. M.S. Gopala Krishna, A.M. Sriramamurthy, and V.M. Radhakrishnan, *Scr. Mater.*, Vol 35 (No. 11), 1996, p 1325
9. F. Dobes and K. Millicka, *Met. Sci.*, Vol 10, 1976, p 382
10. K.G. Samuel, S.L. Mannan, and V.M. Radhakrishnan, *Trans. Indian Inst. Met.*, Vol 46 (No. 3), 1993, p 159